AMERICAN SCIENTIFIC PUBLISHERS

Science of Advanced Materials
Vol. 7, pp. 789–793, 2015
(www.aspbs.com/sam)

Piezoelectric, Piezo-Phototronic, and UV Sensing Properties of Single Ultra Long Nanobelt

Jawayria Mujtaba[1], Umair Manzoor[2,*], Sadaf Zia[1], Muhammad Hafeez[1], and Arshad Saleem Bhatti[1]

[1]*Center for Micro and Nano Devices (CMND), Department of Physics, COMSATS Institute of Information Technology, Islamabad, 44000, Pakistan*
[2]*Alamoudi Water Chair, King Saud University, Riyadh, 11451, Saudi Arabia*

ABSTRACT

We present proof-of-concept of a potential new single ZnO nanobelt based sensor for converting piezoelectric effect in to visible light. Mechanical stress on ZnO ultra-long nanobelts was generated by bending at different angles and systematic color change was observed. IV curves suggested significant change in the electrical properties with applied stress. As-constructed single nanobelt UV sensor exhibit good sensitivity, indicating that these structures can be a promising candidate for miniaturization of proposed device and UV irradiation monitoring in many areas.

KEYWORDS: Sn Doping, Nanostructures (ZnO), Piezoelectric Effect, Optical and Electrical Properties.

1. INTRODUCTION

ZnO exhibits dual properties of semiconductor and piezoelectricity. This amazing property of ZnO is because of its crystal structure, which has tetrahedrally bonded oxygen atoms and zinc atoms.[1] The coupling of electrical, optoelectronic and photochemical properties of ZnO give a unique combination for future applications in chemical, biology, aerospace, military, and medical technologies. The interest in this material is also fueled by its prospects in optoelectronics applications.[2] ZnO nanostructures are very promising candidates for piezoelectricity.[3] This scientific interest is mainly explained by the enhancement of some properties already present in the bulk material. As an example, the piezoelectric coefficient d_{33} is higher in mono or bi-dimensional structures such as nanobelts than in the bulk material.[4] Different research groups in their independent studies, suggested change in electric properties with applied stress in pure and doped ZnO.[5–9]

Piezoelectricity is important for advance applications but mechanical action, however, is not easy to be interfaced directly with silicon technologies without innovative design and approaches. The aim of this work is to provide, for the first time to the best of our knowledge, a comprehensive experimental study on the change in color and electrical properties of Sn-doped ZnO ultra-long nanobelt, as a result of applied stress. After an overview on the morphology, structural and optical properties, florescent optical microscopy images, IV characterization and UV sensing capability are reported.

2. EXPERIMENTAL PROCEDURE

ZnO nanobelts were fabricated by simple vapor transport method. Ball milled mixture of Zinc Oxide powder (99.9%, Hayashi Pure Chemical Industries, Osaka, Japan) and Graphite, in 1:1 weight ratio, was used as catalyst. Milling and mixing of ZnO and C was done in planetry ball mill (Fritsch, Germany) for 25 hours at 200 rpm. 0.2 g of SnO was added in 0.8 g of ZnO and C mixture (source material) for doping. Alumina boat was loaded with source material and Si substrates were placed on top of the boat. The boat was then placed at the center of the tube furnace inside a quartz tube (ϕ35 mm). The furnace temperature was set at 1030 °C for 30 minutes and ramp rate was 10 °C/minute. Ar gas mixed with a small amount of oxygen was used as a carrier gas.

Scanning electron microscope (SEM, Hitachi SU-1500) was used for morphology and crystal structure of as-grown products were characterized by X-ray diffraction (XRD, PANalytical X-pert Pro with Cu-Kα radiations). UV-VIS spectroscope (Perkin Elmer Lambda 950) was used for spectroscopic studies and florescence images were taken using optical microscope (Olympus BX61).

2 mm steel wire was cut into 1.5 inch pieces and non-conductive tape (sticky on both sides) was wrapped on the wire. ZnO ultralong belts were shifted on a glass slide and then wire, with tape, was gently pressed against the glass slide in such a way that both wire and the belts are parallel to each other. The wire was then bent by applying force by

*Author to whom correspondence should be addressed.
Email: umanzoor@ksu.edu.sa
Received: 27 January 2014
Accepted: 19 March 2014

ARTICLE

hand. The same wire was bent at different angles to measure optical and electrical properties at different angles.

3. RESULTS AND DISCUSSION

We used a mixture of ZnO and SnO powders in a weight ratio of 4:1 as the source material to grow Sn-doped ZnO nanobelts. It is known that SnO decompose into Sn and O_2 at high temperature, therefore no catalyst was used. Figure 1(a) is SEM image of Sn-doped ZnO Nanobelts. The image clearly suggests two distinct sizes of Nanobelts; Majority had smaller dimensions with width of 12.38 μm $\pm$ 4.38 μm and thickness 519.12 nm $\pm$ 20.6 nm. Larger size belts are few in number but ultra-long, with length more than 0.5 mm, in most of the cases. One such as-synthesized belt is shown in Figure 1(b). The inset clearly suggested belt shape rectangular morphology. Figure 1(c) is the XRD pattern, clearly suggesting phase pure ZnO with high crystalinity. EDX results are shown as inset in Figure 1(c). Zn, O and Sn peaks are clearly visible, suggesting that Sn is present in significant amount in the sample. Figure 1(d) is SEM image showing ultralong nanobelts, isolated from the bulk, by scratching from the substrate (using very sharp knife) and placing it on a glass piece with few drops of ethanol. ZnO Nanobelts were then sticked on non-conducting PVA tape wrapped around a steel wire (ϕ2 mm). In short, Figure 1 is a clear indication that ultralong, highly crystalline, phase pure ZnO nanobelts can be synthesized and isolated on a nonconducting tape.

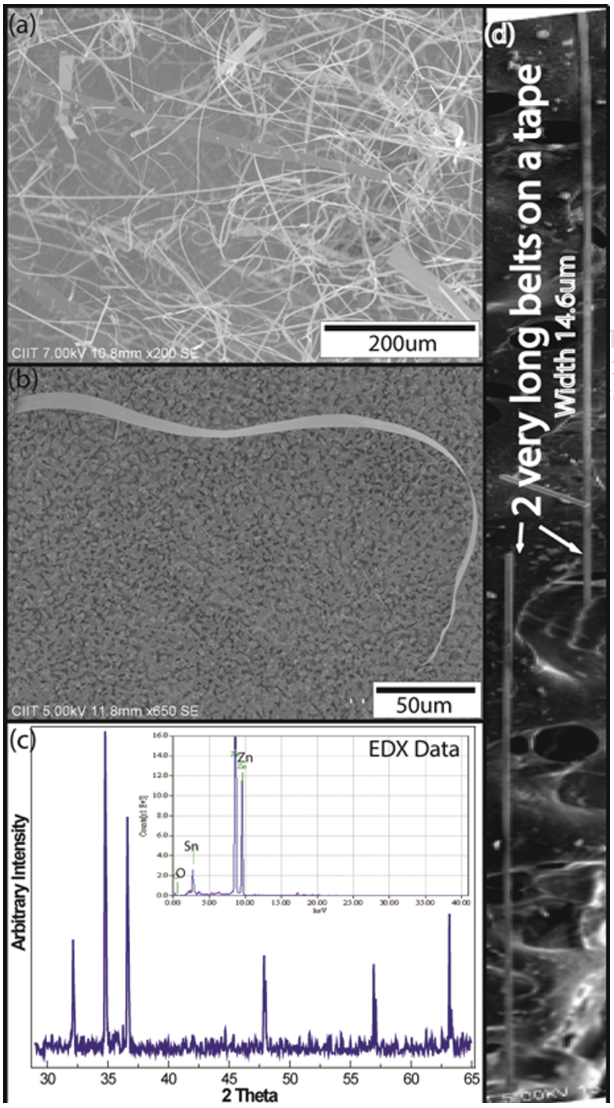

Fig. 1. (a) low magnification image of as-synthesized Sn-doped ZnO Nanobelts. The image clearly suggests two distinct sizes of Nanobelts. (b) SEM image of a complete nanobelt. The inset SEM image is the cross sectional view, conforming belt shape morphology. (c) XRD data shows only ZnO peaks, clearly indicting phase pure ZnO (d) SEM image of ultralong ZnO nanobelt on a non-conducting tape.

Figure 2(a) shows the UV-Vis transmittance spectra taken at room temperature. The line is not very uniform indicating that light may be scattered but overall signal to noise ratio is good. The direct band emission (major peak in UV range) is wide. It is expected that dopant atoms enter substitutionally into the zinc sites in the ZnO lattice so that they act as ionized donors (different oxidation states).[1] Therefore, it is likely to be associated with oxygen deficiencies. The donor electrons occupy the states at the bottom of the conduction band (C.B.) and the bandgap widens.

The intensity of green emission (visible range) can be enhanced by increasing the number of oxygen vacancies, and this was done by doping of Sn in ZnO nanowires.[2] Native or intrinsic defects (two minor peaks in the visible range) are due to imperfections in the crystal lattice that involve the constituent elements. Understanding the incorporation and behavior of point defects in ZnO is essential to its successful application in devices. Defects are often electrically active and introduce levels in the band gap of the semiconductor, which involve transitions between different charge states of the same defect[3] and these transition levels are observable quantities that can be derived and estimated.

Figure 2(b) shows the FTIR spectrum of Sn-doped ZnO nanobelts. Metal oxides generally give absorption bands below 1000 cm^{-1} arising from interatomic vibrations. The bands around 418 cm^{-1} and 572 cm^{-1} corresponds to Zn–O and Sn–O bonds respectively.[4] Wide band at 3400 cm^{-1} indicates the presence of water. The bands at 3400 cm^{-1} and 1620 cm^{-1} are due to adsorption of humidity.[5] One reasonable explanation and possibility of these peaks are because all the optical characterization was performed in ambient conditions.

ZnO is a Piezophototronic material. The existence of "piezo-charges" at the interface introduce three possible effects[6] and one of the most important is the shift in local electronic band structure due to the introduced local potential. By carefully controlling the bending of the

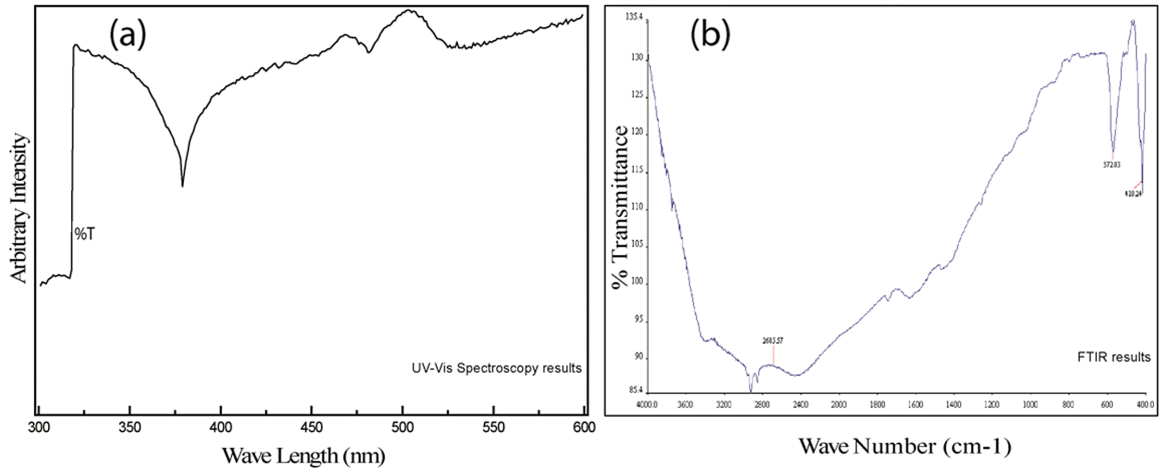

Fig. 2. UV-Vis spectra (a) shows direct band emission in the UV range and 2 minor defect related peaks in the visible range. (b) is the FTIR spectra of Sn-doped ZnO Nanobelts.

nanobelt, local applied pressure can be varied resulting in a systematic control of electronic band structure. In our case, by carefully controlling the bending of nanobelt, optical emissions can be controlled in the visible range. In this report, ZnO was deliberately doped with SnO to observe optical emissions in visible range. When the nanobelt was bended at different angles, the local applied pressure was different, subsequently effecting electronic band structure which result in different colors in the visible region.[7] Figures 3(i) and (ii) is the clear demonstration of this effect. Selected part of the nanobelt (with significant color change upon bending) is shown. Images (a∼d) is bending on one side and image (e∼f) shows the same belt after bending in the opposite direction. Li and his group suggested a relationship between band gap and biaxial tensile stress[8] as follows:

$$E_g = 3.171 + 0.027\sigma_{xx}$$

This again is an indication that bandgap of ZnO is related to the stress and changes with the applied stress. The slight difference in colors after bending in opposite directions (but similar angles) as shown in Figures 3(i)-(b) and (f) is may be because, the positive piezoelectric charges lower the energy band and the negative piezoelectric charges raise the energy band in *n*-type semiconductors. This effect can also be related to crude experimental conditions but repeated experiments show similar behavior and clearly ruled out the possibility of the experimental error. It is also interesting to note that the results are reproducible with all Sn-nanobelts.

During the bending process, the *I*–*V* characteristics of the belt were monitored. Six typical bending curvatures of the ZnO NW are shown in SEM images in Figures 3(a)–(f), and their corresponding *I*–*V* curves are presented in Figure 4. The symmetric shape of the *I*–*V* curves indicates good ohmic contacts at both ends of the belt. The current drops significantly with increased

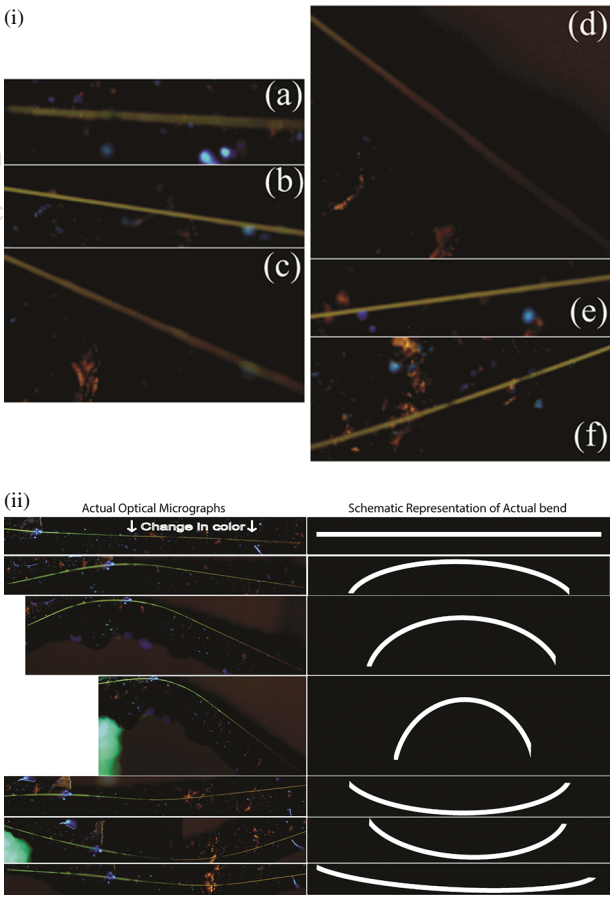

Fig. 3. (i) Optical micrograph florescent images (selected part) of Sn-doped ZnO Nanobelt after bending at different angles. The color change is clearly visible with different bending angles. (ii) Optical micrograph full length florescent images of Sn-doped ZnO Nanobelt after bending at different angles. The color change is clearly visible with different bending angles. The schematics clearly suggesting the bending angles are also shown against each bend.

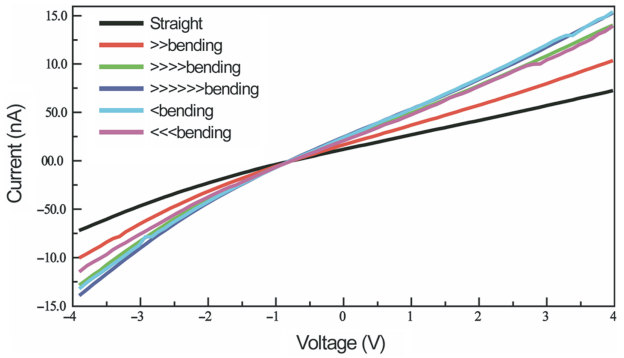

Fig. 4. IV curves of Sn-doped ZnO Nanobelt after bending at different angles. The results clearly suggested increase in conductance with subsequent bending.

bending (Figs. 4(b∼e)), indicating decreased conductance with increased strain. The mechanism of the conduction can be described by the following equation:[9]

$$SnO_{2ZnO} \rightarrow Sn''_{Zn} + O^{x}_{O} + \frac{1}{2}O_2 + 2e'$$

Sn^{+4} ions substituted Zn^{2+} ions in the lattice induce positive charges in the material. In order to maintain electrical neutrality, two negative electrons are induced to compensate the excess positive charges. When a small strain was applied on nanobelt by bending the steel wire, the current increased, further systematic increase was observed with the subsequent increase in the bending angles. Similar behavior was observed when same nanobelt was bended in the opposite direction. In short, we observed a bending-induced enhancement in conductance. Bending can change the band structure and this effect is also demonstrated in Figure 3. Bending induces outer tensile and inner compressive strains and thus the combination of this and its effect is very complex. Han and co-workers discussed this issue in detail suggesting that tensile strain and shear strain tend to narrow the band gap, since their states are much lower than the compressive states.[10] The free electron carriers will be mainly distributed in the lower sub-bands and thus increasing the conductivity. The florescence microscopy results (Fig. 3) are in perfect agreement with each other and the color change with subsequent bending was from lower to higher wavelengths suggesting decrease in the bandgap. However, some of the research groups[4] suggested bending-induced decrease in conductance (opposite effect).

The low-conductance state can represent the off ("0") state, and the high conductance the on ("1") state. Therefore, modulation of the conductance in ZnO NWs via bending can be used as a nanoscale switch or other electromechanical device in nanoelectromechanical systems (NEMS). However, this is relatively a new field and more experiments and indepth theoretical calculations are required to reveal the underlying complex mechanisms.

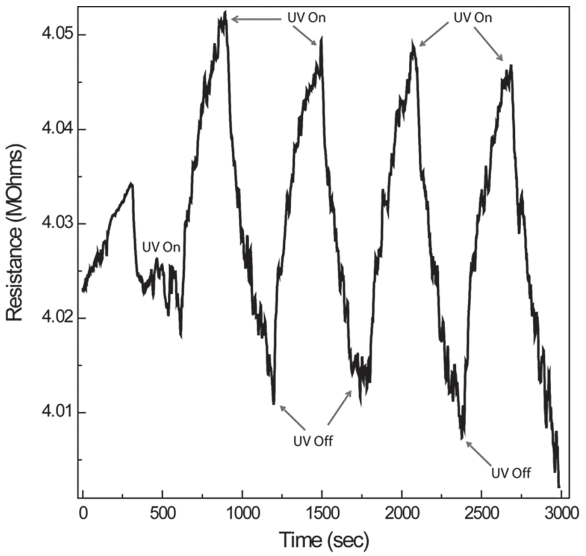

Fig. 5. UV sensing result of a single belt. The first cycle was with low UV intensity and intensity was doubled for next 4 cycles. The results clearly suggest that Sn-doped ZnO Nanobelt can be used as an effective UV sensor.

The photosensing properties were characterized at room temperature in air. When Sn-doped ZnO nanobelt was exposed to UV, electrons transition takes place from the valence band to the conduction band, giving rise to a current flow and decrease in the resistance. Figure 5 shows UV sensing results of a single belt. In the 1st cycle UV intensity was low and it was doubled for the next 4 cycles. However, overall sensitivity was low and the response time was also slow. Different researchers explained the decay process by different mechanisms. For example, Lupan et al. reported that the decay process can be attributed to the recombination of electron–hole pairs and the readsorption of oxygen molecules on the surface.[11] He et al. suggested that the decay is mainly determined by the electron free-carrier recombination and molecules adsorption on the surface.[12] Cheng et al. reported that when the UV illumination was removed, the photocurrent fell from the maximum fast at the first stage, which indicates the rapid loss of electrons in the conduction band via retrapping the electrons. Then the slow falling of the current to the initial value can be attributed to the reabsorbed oxygen on the ZnO which decreases its conductivity.[13] However, the decay mechanism needs further discussion.

4. CONCLUSION

In summary, a possible concept that piezoelectric effect in Sn-doped ZnO ultra-long nanobelts can be measured by change in color was experimentally demonstrated. There was a systematic change in color and electrical properties with change in bending angle. One reasonable explanation is that because of the applied stress there is a modification in the local band structure. This change in the bandgap is

responsible not only for the change in electrical properties but also change in the color. Sn was doped in ZnO to create defects which are responsible of emitting radiations in the visible range under florescence microscope. XRD and SEM confirmed phase pure ZnO and belt shape morphology respectively. The as-constructed single nanobelt sensor exhibit good sensitivity towards UV irradiation, indicating that these sensors can be a promising candidate for miniaturization of device and UV irradiation monitoring in advance applications.

Acknowledgment: This project was supported by NSTIP strategic technologies program number (12-WAT-2451-02) in the Kingdom of Saudi Arabia.

References and Notes

1. U. Ozgur, Y. I. Alivov, C. Liu, A. Teke, M. A. Reshchikov, S. Dogan, V. Avrutin, S.-J. Cho, and H. Morkoc, *J. Appl. Phys.* 98, 1 **(2005)**.
2. U. Manzoor and D. K. Kim, *Scripta Mater.* 54, 807 **(2006)**.
3. S. Xu and Z. Wang, *Nano Research* 4, 1013 **(2011)**.
4. X. Xudong, J. Zhou, H. Jin, J. Liu, N. Xu, and Z. L. Wang, *Nano Lett.* 6, 2768 **(2006)**.
5. K.-H. Kim, B. Kumar, K. Y. Lee, H.-K. Park, J.-H. Lee, H. H. Lee, H. Jun, D. Lee, and S.-W. Kim, *Nature* 3, 2017 **(2012)**.
6. B. Kumar and S. W. Kim, *Nano Energy* 1, 342 **(2012)**.
7. M. Y. Choi, D. Choi, M. J. Jin, I. Kim, S. H. Kim, J. Y. Choi, S. Y. Lee, J. M. Kim, and S. W. Kim, *Adv. Mater.* 21, 2185 **(2009)**.
8. A. Onodera, N. Tamaki, Y. Kawamura, T. Sawada, and H. Yamashita, *Jpn. J. Appl. Phys.* 35, 5160 **(1996)**.
9. J. Wang, W. Chen, and M. Wang, *J. Alloys Compd.* 449, 44 **(2008)**.
10. B. E. Sernelius, K. F. Berggren, Z. C. Jin, I. Hamberg, and C. G. Granqvist, *Phys. Rev.* 37, 10244 **(1988)**.
11. S. Zia, M. Amin, U. Manzoor, and A. S. Bhatti, *Applied Physics A: Materials Science and Processing* 115, 275 **(2013)**.
12. Electronic Properties of Defects, In Fundamentals of Semiconductors, Springer, Berlin, Heidelberg **(2001)**, pp. 159–202.
13. F. Gu, S. F. Wang, C. F. Song, M. K. Lü, Y. X. Qi, G. J. Zhou, D. Xu, and D. R. Yuan, *Chem. Phys. Lett.* 372, 451 **(2003)**.